



Hayes, S., Sharma, A., Fraser, D., Trevisan, M., Cragg-Barber, C. W. K., Tavridou, E., Fankhauser, C., Jenkins, G., & Franklin, K. (2017). UV-B perceived by the UVR8 photoreceptor inhibits plant thermomorphogenesis. *Current Biology*, 27(1), 120-127.
<https://doi.org/10.1016/j.cub.2016.11.004>

Publisher's PDF, also known as Version of record

License (if available):
CC BY

Link to published version (if available):
[10.1016/j.cub.2016.11.004](https://doi.org/10.1016/j.cub.2016.11.004)

[Link to publication record in Explore Bristol Research](#)
PDF-document

This is the final published version of the article (version of record). It first appeared online via Elsevier (Cell Press) at [http://www.cell.com/current-biology/abstract/S0960-9822\(16\)31329-X](http://www.cell.com/current-biology/abstract/S0960-9822(16)31329-X). Please refer to any applicable terms of use of the publisher.

University of Bristol - Explore Bristol Research

General rights

This document is made available in accordance with publisher policies. Please cite only the published version using the reference above. Full terms of use are available:
<http://www.bristol.ac.uk/red/research-policy/pure/user-guides/ebr-terms/>

Current Biology

UV-B Perceived by the UVR8 Photoreceptor Inhibits Plant Thermomorphogenesis

Highlights

- UVR8 activity inhibits auxin signaling and stem elongation at high temperature
- UVR8 acting with COP1 suppresses transcript abundance of the bHLH factor PIF4
- UV-B-mediated degradation of PIF4 is temperature dependent
- UV-B stabilizes the bHLH factor HFR1, which can bind to and inhibit PIF4 function

Authors

Scott Hayes, Ashutosh Sharma,
Donald P. Fraser, ...,
Christian Fankhauser,
Gareth I. Jenkins, Keara A. Franklin

Correspondence

kerry.franklin@bristol.ac.uk

In Brief

Hayes et al. show that low-dose UV-B, perceived by the UVR8 photoreceptor, is a potent inhibitor of high-temperature-induced stem elongation. This provides plants with an important braking mechanism in bright sunlight, preventing excessive elongation growth that could lead to stem lodging and critical reductions in root and leaf biomass.

UV-B Perceived by the UVR8 Photoreceptor Inhibits Plant Thermomorphogenesis

Scott Hayes,^{1,2,6} Ashutosh Sharma,^{1,6} Donald P. Fraser,¹ Martine Trevisan,³ C. Kester Cragg-Barber,¹ Eleni Tavridou,⁴ Christian Fankhauser,³ Gareth I. Jenkins,⁵ and Keara A. Franklin^{1,7,*}

¹School of Biological Sciences, Life Sciences Building, University of Bristol, Bristol BS8 1TQ, UK

²Plant Ecophysiology, Institute of Environmental Biology (IEB), Utrecht University, Padualaan 8, 3584 Utrecht, the Netherlands

³Centre for Integrative Genomics, Faculty of Biology and Medicine, University of Lausanne, 1015 Lausanne, Switzerland

⁴Department of Botany and Plant Biology, University of Geneva, Sciences III, 30 Quai E. Ansermet, 1211 Geneva 4, Switzerland

⁵Institute of Molecular, Cell and Systems Biology, College of Medical, Veterinary and Life Sciences, University of Glasgow, Glasgow G12 8QQ, UK

⁶Co-first author

⁷Lead Contact

*Correspondence: kerry.franklin@bristol.ac.uk

<http://dx.doi.org/10.1016/j.cub.2016.11.004>

SUMMARY

Small increases in ambient temperature can elicit striking effects on plant architecture, collectively termed thermomorphogenesis [1]. In *Arabidopsis thaliana*, these include marked stem elongation and leaf elevation, responses that have been predicted to enhance leaf cooling [2–5]. Thermomorphogenesis requires increased auxin biosynthesis, mediated by the bHLH transcription factor PHYTOCHROME-INTERACTING FACTOR 4 (PIF4) [6–8], and enhanced stability of the auxin co-receptor TIR1, involving HEAT SHOCK PROTEIN 90 (HSP90) [9]. High-temperature-mediated hypocotyl elongation additionally involves localized changes in auxin metabolism, mediated by the indole-3-acetic acid (IAA)-amido synthetase Gretchen Hagen 3 (GH3).17 [10]. Here we show that ultraviolet-B light (UV-B) perceived by the photoreceptor UV RESISTANCE LOCUS 8 (UVR8) [11] strongly attenuates thermomorphogenesis via multiple mechanisms inhibiting PIF4 activity. Suppression of thermomorphogenesis involves UVR8 and CONSTITUTIVELY PHOTOMORPHOGENIC 1 (COP1)-mediated repression of *PIF4* transcript accumulation, reducing PIF4 abundance. UV-B also stabilizes the bHLH protein LONG HYPOCOTYL IN FAR RED (HFR1), which can bind to and inhibit PIF4 function. Collectively, our results demonstrate complex crosstalk between UV-B and high-temperature signaling. As plants grown in sunlight would most likely experience concomitant elevations in UV-B and ambient temperature, elucidating how these pathways are integrated is of key importance to the understanding of plant development in natural environments.

RESULTS AND DISCUSSION

Growth in stressful environments, such as high temperature and vegetational shade, can trigger plant acclimation/escape

responses involving rapid stem elongation at the expense of biomass production [12, 13]. A number of studies have identified molecular crosstalk between high temperature and light signaling via the red/far-red light-absorbing phytochrome photoreceptors [13]. More recently, cryptochrome 1 has been shown to physically interact with phytochrome-interacting factor 4 (PIF4) [14, 15] to regulate high-temperature-mediated hypocotyl elongation in blue light [14]. Although daily peaks in ultraviolet-B light (UV-B) levels correlate with temperature maxima in natural photoperiods [16], the integration of UV-B and thermomorphogenesis signaling pathways has remained largely unexplored. Following UV-B absorption, UV resistance locus 8 (UVR8) monomerizes and binds to the E3 ubiquitin ligase constitutively photomorphogenic 1 (COP1) to initiate downstream signaling [11].

Here we show that low-dose UV-B provides a strong brake on high-temperature-induced hypocotyl elongation in seedlings (Figure 1A) and petiole elongation in adult plants (Figures 1B and 1C). UV-B-mediated inhibition of hypocotyl elongation at high temperature was observed in continuous light, 16 hr photoperiods, and 8 hr photoperiods, suggesting no photoperiodic specificity to the response (Figures 1A, S1A, and S1B). Considerable high-temperature-mediated stem elongation responses were observed in the *uvr8-1* mutant in the presence of UV-B, demonstrating that the inhibition effects observed are predominantly photomorphogenic responses mediated by UVR8 (Figures 1A–1C). Some UVR8-independent, UV-B-mediated inhibitions of hypocotyl and petiole elongation were, however, recorded. In addition to changes in petiole length, a UVR8-mediated suppression of high-temperature-induced leaf hyponasty was observed in UV-B (Figure S1C). UV-B treatment decreased leaf area independently of UVR8 at 20°C and 28°C. A smaller decrease was observed following high-temperature treatment in wild-type (WT) plants, but not in *uvr8* mutants. When UV-B and temperature were applied simultaneously, elevated temperature rescued the small leaf phenotype induced by UV-B in a UVR8-dependent manner (Figure S1D). UV-B-induced reductions in leaf area are complex and likely to involve stress signaling pathways in addition to UVR8 signaling [17]. Leaf area phenotypes may therefore reflect enhanced repair of UV-B-induced DNA damage at high temperature [18, 19].

Transfer of plants to high temperature transiently increases *PIF4* transcript abundance [6–8, 20] and promotes the

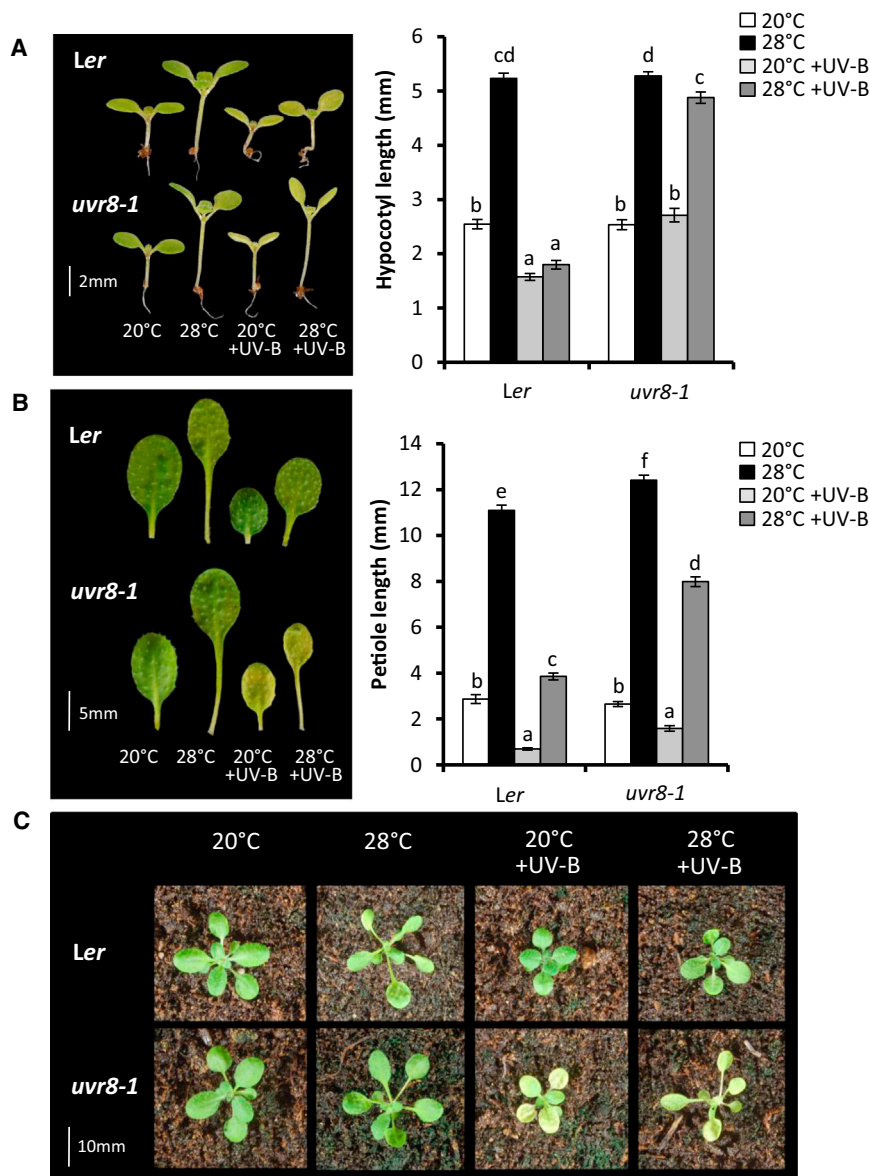


Figure 1. UV-B Perceived by UVR8 Inhibits High-Temperature-Induced Architectural Adaptations in Arabidopsis

(A) Hypocotyl lengths of *Ler* and *uvr8-1* seedlings grown in continuous light for 3 days at 20°C, before transfer to 20°C, 28°C, 20°C + UV-B, or 28°C + UV-B for a further 4 days. Data represent mean length (n = 40) ± SE.

(B) Petiole length of leaf 4 of *Ler* and *uvr8-1* plants grown for 10 days in 16 hr light/8 hr dark cycles at 20°C before transfer to 20°C, 28°C, 20°C + UV-B, or 28°C + UV-B for a further 9 days. Data represent mean length (n ≥ 23) ± SE. Different letters indicate statistically significant means (p < 0.05). Two-way ANOVA confirmed that there was a significant interaction between genotype and condition on petiole length (p < 0.001).

(C) Representative rosettes of plants grown as in (B).

See also Figure S1.

UV-B-mediated suppression of auxin biosynthesis/signaling genes was dependent upon the presence of UVR8, confirming the response to be photomorphogenic (Figure 2B). No high-temperature-mediated increase in *IAA29* transcript was observed in *pi4* mutants. *PIF4* overexpressor seedlings displayed elevated levels of *IAA29* transcript, which were suppressed by UV-B (Figure S1E).

UV-B has previously been shown to inhibit auxin biosynthesis in simulated canopy shade (low red-to-far red ratio light; low R:FR), by promoting *PIF4*/*PIF5* degradation and stabilizing DELLA proteins [27]. The latter inhibit *PIF* function through heterodimerization [28, 29]. We therefore analyzed the stability of constitutively expressed, hemagglutinin (HA)-tagged *PIF4* in our conditions. In agreement with previous observations at 20°C,

accumulation of phosphorylated *PIF4* protein [12]. In diurnal cycles, warm temperatures inhibit the transcriptional regulator EARLY FLOWERING 3 (ELF3), relieving *PIF4* repression at night [21–23]. *PIF4* promotes the expression of auxin biosynthesis genes [8, 24], including *YUCCA8* (*YUC8*), which encodes a key rate-limiting enzyme in tryptophan-dependent auxin biosynthesis [25, 26]. High temperature therefore elevates free indole-3-acetic acid (IAA, the major natural auxin) levels and the expression of auxin-responsive genes, such as *IAA29* [2, 6, 8, 24]. As expected, no significant high-temperature-induced hypocotyl elongation was evident in *pi4* mutants in our conditions (Figure 2A) [6–8]. UV-B strongly suppressed the elongated phenotype of *PIF4* overexpressor seedlings at 20°C and 28°C, suggesting that UV-B may inhibit *PIF4* activity (Figure 2A). In support of this idea, UV-B inhibited the accumulation of *YUC8* and *IAA29* transcript abundance at both temperatures (Figure 2B). Consistent with hypocotyl elongation data (Figure 1A),

UV-B treatment resulted in rapid *PIF4*-HA degradation (Figures 3A and 3B) [27]. Intriguingly, no UV-B-mediated degradation of *PIF4*-HA was observed at 28°C, suggesting a temperature-dependent component to this response (Figures 3A and 3B). We next investigated UV-B-mediated suppression of thermomorphogenesis in a DELLA quintuple mutant, deficient in all DELLA proteins [6]. Despite showing longer hypocotyls than WT plants in all experimental conditions, strong UV-B-mediated inhibition of hypocotyl elongation was observed in *della*-null mutants at high temperature, confirming that UV-B-mediated stabilization of DELLAs does not constitute an underlying regulatory mechanism in the inhibition of thermomorphogenesis (Figure S2A). Together, these data suggest that the dominance of regulatory components controlling UV-B-mediated hypocotyl inhibition differs between thermomorphogenesis and shade avoidance.

We next investigated the effect of UV-B on *PIF4* transcript abundance. UV-B strongly inhibited *PIF4* transcript accumulation at

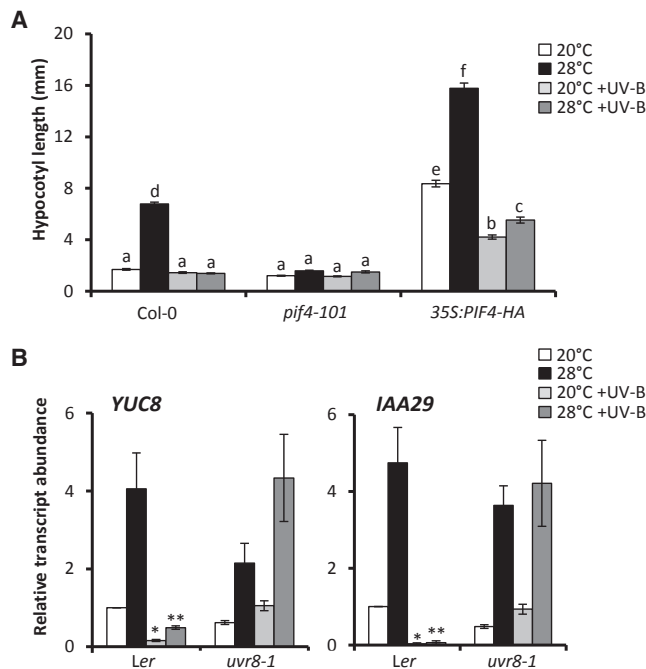


Figure 2. UV-B Perceived by UVR8 Inhibits PIF4 Activity and Auxin Signaling at High Temperature

(A) Hypocotyl lengths of Col-0, *pif4-101*, and 35S:PIF4-HA seedlings grown in continuous light for 3 days at 20°C, before transfer to 20°C, 28°C, 20°C + UV-B, or 28°C + UV-B for a further 4 days ($n \leq 27$; \pm SE). Different letters indicate statistically significant means ($p < 0.05$).

(B) Relative transcript abundance of *YUC8* and *IAA29* in Ler and *uvr8-1* seedlings grown for 10 days in 16 hr light/8 hr dark cycles at 20°C, before transfer at dawn to the indicated conditions for 4 hr ($n = 3$; \pm SE; *significant UV-B-mediated decrease in transcript abundance when compared to 20°C, $p < 0.05$; **significant UV-B-mediated decrease in transcript abundance when compared to 28°C, $p < 0.05$).

See also Figure S1.

20°C and 28°C in a UVR8-dependent manner (Figure 3C). Mutants deficient in the UVR8-binding protein COP1 showed significantly reduced *PIF4* transcript in the absence of UV-B and insensitivity to UV-B treatment at both temperatures (Figure S2B). Such data suggest a fundamental requirement for COP1 in promoting *PIF4* transcript accumulation. Consistent with this observation and previous studies [20], we observed no thermomorphogenesis in *cop1* mutants (Figure S2C). Plants expressing a constitutively dimeric form of UVR8 in the *uvr8-1* background (*uvr8-1*/GFP-UVR8^{W285F}), which is unable to bind COP1 [30], displayed no UV-B-mediated inhibition of thermomorphogenesis (Figure S2D). This supports the hypothesis that UVR8 monomerization and UVR8-COP1 binding is required for this response. The effect of reduced *PIF4* transcript levels on PIF4 protein abundance was investigated by western blotting of native PIF4, using a polyclonal PIF4 antibody. This antibody recognized PIF4 when tested on a range of mutant and transgenic lines (Figure S2E). UV-B treatment strongly decreased PIF4 abundance at both temperatures, suggesting that UVR8-mediated suppression of *PIF4* transcript abundance reduces PIF4 protein (Figure 3D).

The transcriptional regulation of *PIF4* has been shown to involve the regulatory proteins ELF3 and ELONGATED

HYPOCOTYL 5 (HY5) [20, 21]. In day/night cycles, ELF3 suppresses the transcription of *PIF4* in the early evening, promoting PIF4 accumulation and hypocotyl elongation toward the end of the night [23]. As high temperatures suppress ELF3 binding to the *PIF4* promoter [21], it has been proposed that (in short days at least) reduced ELF3-mediated repression of *PIF4* transcript accumulation drives high-temperature-mediated architectural changes. We therefore investigated the consequence of daytime UV-B supplementation on nighttime *PIF4* transcript levels at 20°C and 28°C. Plants were grown in short (8 hr) photoperiods, and *PIF4* levels were quantified throughout the day and early night. In the absence of UV-B, *PIF4* transcript showed the expected early night suppression at 20°C (Figure 3E) [21, 23, 31]. UV-B strongly reduced *PIF4* transcript abundance during the day, maintaining low *PIF4* levels throughout the early night, before eventually reaching similar levels to untreated plants by 8 hr of dark. At 28°C, *PIF4* transcript levels were higher than at 20°C during the early night, consistent with reduced ELF3 function [21]. UV-B treatment still, however, resulted in a sustained suppression of *PIF4* transcript levels across the entire time course (Figure 3F). Despite showing a higher abundance of *PIF4* transcript than WT plants at dawn [21], *elf3-1* mutants displayed UV-B-mediated *PIF4* suppression at both temperatures (Figures S3A and S3B). These data suggest that the inhibition of *PIF4* transcript abundance by UV-B can occur independently of ELF3.

It is likely that UV-B also regulates PIF4 activity at the post-translational level (as evidenced by strong inhibition of hypocotyl elongation in *PIF4* overexpressor seedlings in Figure 2A). ELF3 and HY5 have been shown to inhibit PIF4 activity by direct physical interaction [31] and antagonistic promoter binding [32], respectively. To investigate post-translational regulation by ELF3, we investigated the effect of UV-B on hypocotyl inhibition in *elf3-1* mutants at 20°C and 28°C. Consistent with previous reports, *elf3-1* mutants displayed elongated hypocotyls at 20°C and an exaggerated elongation response to high temperature (Figures 4A and S3C) [21, 31]. These phenotypes were abolished in the presence of UV-B, consistent with a role for UV-B signaling in inhibiting PIF4 function. As UV-B fully inhibited thermomorphogenesis in *elf3* mutants (Figures 4A and S3C), it is unlikely that ELF3 forms a regulatory component of this response. We therefore investigated the role of HY5 and its close relative, HY5 HOMOLOG (HYH). The expression of both is strongly increased in UV-B [33–35]. Single and double *hy5/hyh* mutants displayed significant UV-B-mediated hypocotyl inhibition at 20°C and 28°C (Figure 4B). High-temperature-mediated hypocotyl elongation was completely inhibited by UV-B in WT and *hy5* mutants, suggesting that HY5 is not required for the inhibition response. Conversely, some high-temperature-mediated hypocotyl elongation was observed in *hyh* and *hy5/hyh* mutants in the presence of UV-B, suggesting that HYH contributes to UV-B-mediated thermomorphogenesis inhibition (Figure 4B). No role for HY5 or HYH could be identified in the UV-B-mediated suppression of *PIF4* transcript accumulation (Figure S3D).

The RNA-binding protein FCA has been shown to attenuate hypocotyl elongation at high temperature by promoting the dissociation of PIF4 from *YUC8* chromatin [36]. High temperature increases *FCA* transcript levels 2-fold but does not affect protein stability [36]. A similar high-temperature effect on *FCA*

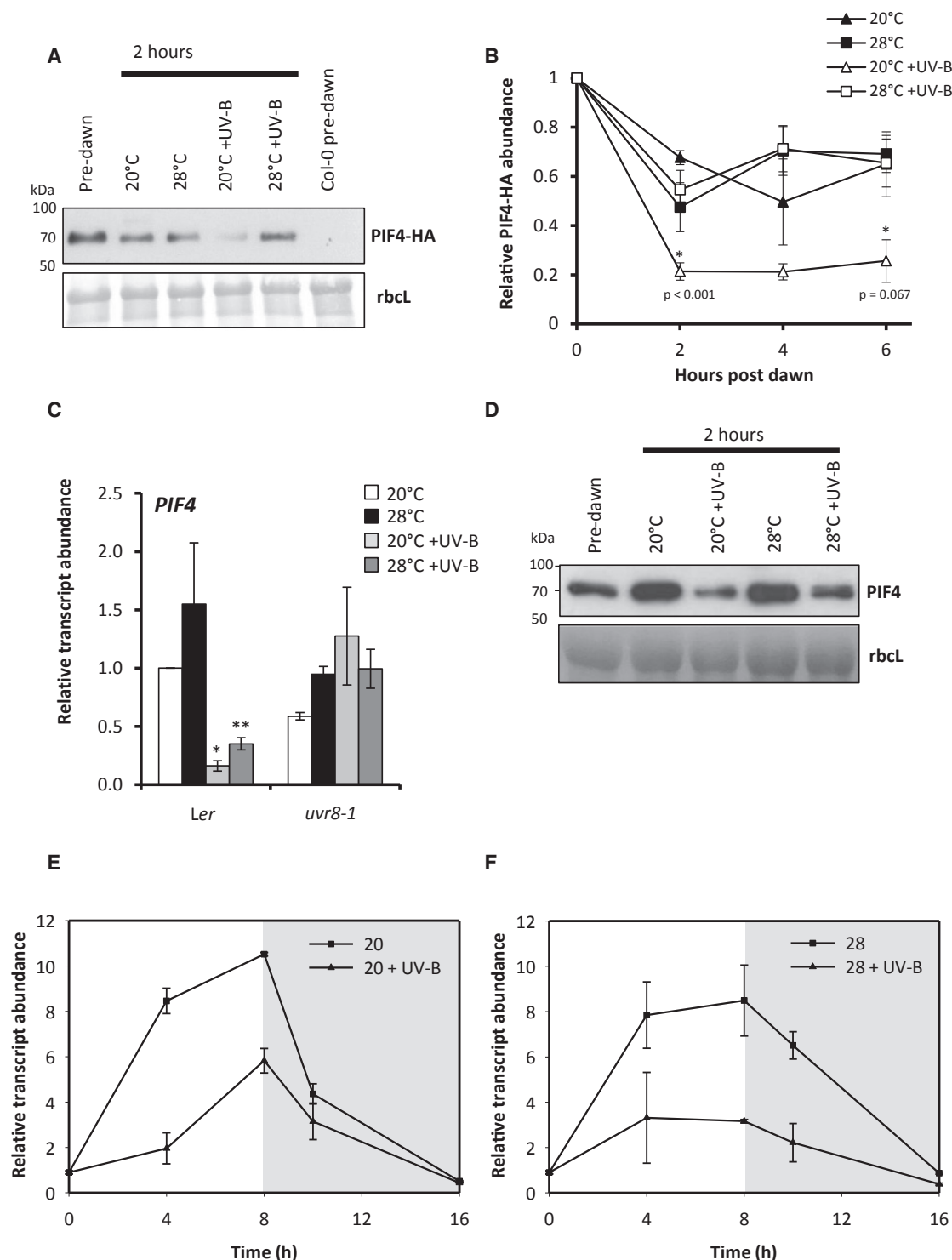


Figure 3. UV-B Inhibits *PIF4* Transcript Accumulation in a *UVR8*-Dependent Manner and Promotes *PIF4* Degradation in a Temperature-Conditional Manner

(A) PIF4-HA abundance in 35S:*PIF4*-HA seedlings grown for 10 days in 16 hr light/8 hr dark cycles at 20°C, harvested before dawn and 2 hr after dawn following transfer to the stated conditions. Col-0 serves as a negative control. Ponceau stain of Rubisco large subunit (rbcL) serves as a loading control.

(B) Time course of plants grown and treated as in (A). Relative protein abundance was normalized to Ponceau staining of the Rubisco large subunit, then expressed as a value relative to pre-dawn levels ($n = 3$; \pm SE). Asterisks denote a significant difference between UV-B- and white light (WL)-treated controls at their respective temperatures.

(legend continued on next page)

transcript levels was observed in our experimental conditions. This was inhibited by UV-B in a UVR8-dependent manner, suggesting that FCA does not form a component of UV-B-mediated hypocotyl inhibition at high temperature (Figure S4A). In low R:FR, PIF function is antagonized in a negative feedback loop by the HLH proteins PHYTOCHROME RAPIDLY REGULATED 1 (PAR1) and PAR2 and the bHLH protein LONG HYPOCOTYL IN FAR RED (HFR1), which form competitive heterodimers unable to bind DNA [37–39]. Inhibition of PIF4 activity by HFR1 has also been reported in monochromatic FR and blue light [12, 40]. Mutants deficient in PAR2 (*par2-1*) displayed exaggerated hypocotyl elongation at high temperature, suggesting a role for PAR2 in the suppression of this response in white light (Figure S4B). Despite this, both *par2-1* and transgenic plants containing reduced transcripts of both *PAR1* and *PAR2* (*PAR1 RNAi*) [39] displayed full UV-B-mediated inhibition of thermomorphogenesis, suggesting neither to be essential for this response (Figure S4B). Indeed, UV-B perceived by UVR8 strongly inhibited *PAR1* and *PAR2* transcript accumulation (Figures S4C and S4D), consistent with their roles as PIF4 target genes.

A partial inhibition of thermomorphogenesis was, however, observed in *hfr1* mutants in the presence of UV-B, suggesting a regulatory role for this protein (Figure 4C). In agreement with previous observations, *HFR1* transcript abundance increased significantly at high temperature (Figure S4E) [12] but was strongly suppressed by UV-B in a UVR8-dependent manner (Figure S4E), consistent with the role of *HFR1* as a PIF4 target gene [38]. We therefore investigated the effect of UV-B on *HFR1* protein stability. *HFR1* levels increased following transfer to high temperature (Figure 4D) [12] and were strongly stabilized by UV-B (Figure 4D). It is possible that *HFR1* binding protects PIF4 from UV-B-induced degradation. Collectively, our data suggest that UV-B-mediated stabilization of *HFR1* contributes to the suppression of PIF4 activity and inhibition of hypocotyl elongation in these conditions.

Conclusions

Here we demonstrate that UV-B is a potent inhibitor of plant thermomorphogenesis (summarized in Figure 4E). Low-dose UV-B supplementation promoted the degradation of PIF4 protein at 20°C, but not 28°C. At high temperature, UV-B, perceived by UVR8, strongly inhibited *PIF4* transcript accumulation, resulting in low PIF4 levels and reduced expression of auxin biosynthesis/signaling genes. No role for the characterized PIF4 transcriptional regulators ELF3 or HY5 [20, 21] could be identified in this response. In the absence of COP1, *PIF4* transcript levels remained low and insensitive to UV-B, suggesting a role for this protein in regulating *PIF4* transcript abundance. Reduced *PIF4* transcript has also been reported in *de-etiolated 1* (*det-1*) mutants, deficient in an enhancer of COP1 activity [20]. Mutants

deficient in COP1 do not elongate at high temperature [20] (Figure S2B), so the role of COP1 in the UV-B-mediated inhibition of this response could not be directly tested. GFP-UVR8^{W285F} plants express a constitutively dimerized UVR8 in the *uvr8-1* background, which is unable to bind COP1 and initiate photomorphogenic signaling [30]. High-temperature-mediated hypocotyl elongation was similar in UV-B-treated GFP-UVR8^{W285F} and *uvr8* mutants, suggesting that UVR8 inhibits thermomorphogenesis via its established photoreceptor activity.

UV-B-mediated suppression of hypocotyl elongation in *PIF4* overexpressor plants suggested that UVR8 inhibits PIF4 activity in addition to repressing transcript abundance. Two recent studies have shown that CRY1 and CRY2 physically interact with PIF4 in blue light to inhibit thermomorphogenesis and shade avoidance [14, 15]. By contrast, UVR8 appears not to physically interact with PIFs [27]. UVR8 does, however, directly interact with COP1 [11]. It is possible that in the presence of UV-B, UVR8 sequesters COP1, reducing its E3 ubiquitin ligase activity and enabling the accumulation of PIF4-negative regulators. Mutant analyses showed that the majority of known PIF4 inhibitors (DELLAs, ELF3, HY5, and PARs) does not have a dominant role in UVR8-mediated inhibition of thermomorphogenesis [28, 29, 31, 32, 39], although we cannot rule out functional redundancy between these regulators. Intriguingly, some role was identified for HYH, highlighting different regulatory capabilities between HY5 and HYH in these conditions. The mechanism by which HYH inhibits PIF4 function is unclear, but it may compete for *PIF4* target promoters at higher temperatures. A clear role was, however, identified for *HFR1*, which is known to antagonize high-temperature-mediated elongation growth in blue light [12]. High temperature and UV-B both stabilized *HFR1* protein, which can inhibit PIF4 activity through heterodimer formation [38]. It is therefore likely that high *HFR1* levels contribute to the UV-B-mediated suppression of thermomorphogenesis.

Collectively, our data support the existence of an overarching mechanism through which UV-B inhibits hypocotyl elongation in *Arabidopsis*. This involves the repression of PIF abundance and activity, which subsequently prevents the upregulation of auxin biosynthesis. The relative contributions of different regulatory components do, however, appear to change with environmental context [27]. Here we show that the molecular mechanisms controlling UV-B-mediated suppression of hypocotyl elongation vary with growth temperature. UVR8/COP1-mediated suppression of *PIF4* transcript accumulation appears to strongly inhibit PIF4 protein accumulation at 20°C and 28°C (Figures 3C–3F and S2B). PIF4 protein is additionally degraded by UV-B treatment at cooler temperatures (Figures 3A and 3B) [27]. At 28°C, PIF4 protein is protected from UV-B-induced degradation (Figures 3A and 3B) but has severely reduced function. We hypothesize that this results, at least in part, from high *HFR1* levels in

(C) *PIF4* transcript abundance in *Ler* and *uvr8-1* seedlings grown as in (A) and harvested at 4 hr (*significant UV-B-mediated decrease in transcript abundance when compared to 20°C, $p < 0.05$; **significant UV-B-mediated decrease in transcript abundance when compared to 28°C, $p < 0.05$).

(D) Representative blot showing PIF4 abundance in *Ler* grown as in (A) at the 2 hr time point using anti-PIF4 antibody. Ponceau stain of Rubisco large subunit (rbcl) serves as a loading control.

(E and F) Time course of *PIF4* transcript abundance. Seedlings were grown for 10 days in 8 hr light/16 hr dark cycles at 20°C. On day 11, plants were transferred to either (E) 20°C or (F) 28°C ± UV-B. UV-B treatment was maintained for the duration of the photoperiod and plants harvested at the times shown. All values are normalized to time 0. The mean of two biological repeats are shown ± SD.

See also Figures S2 and S3.

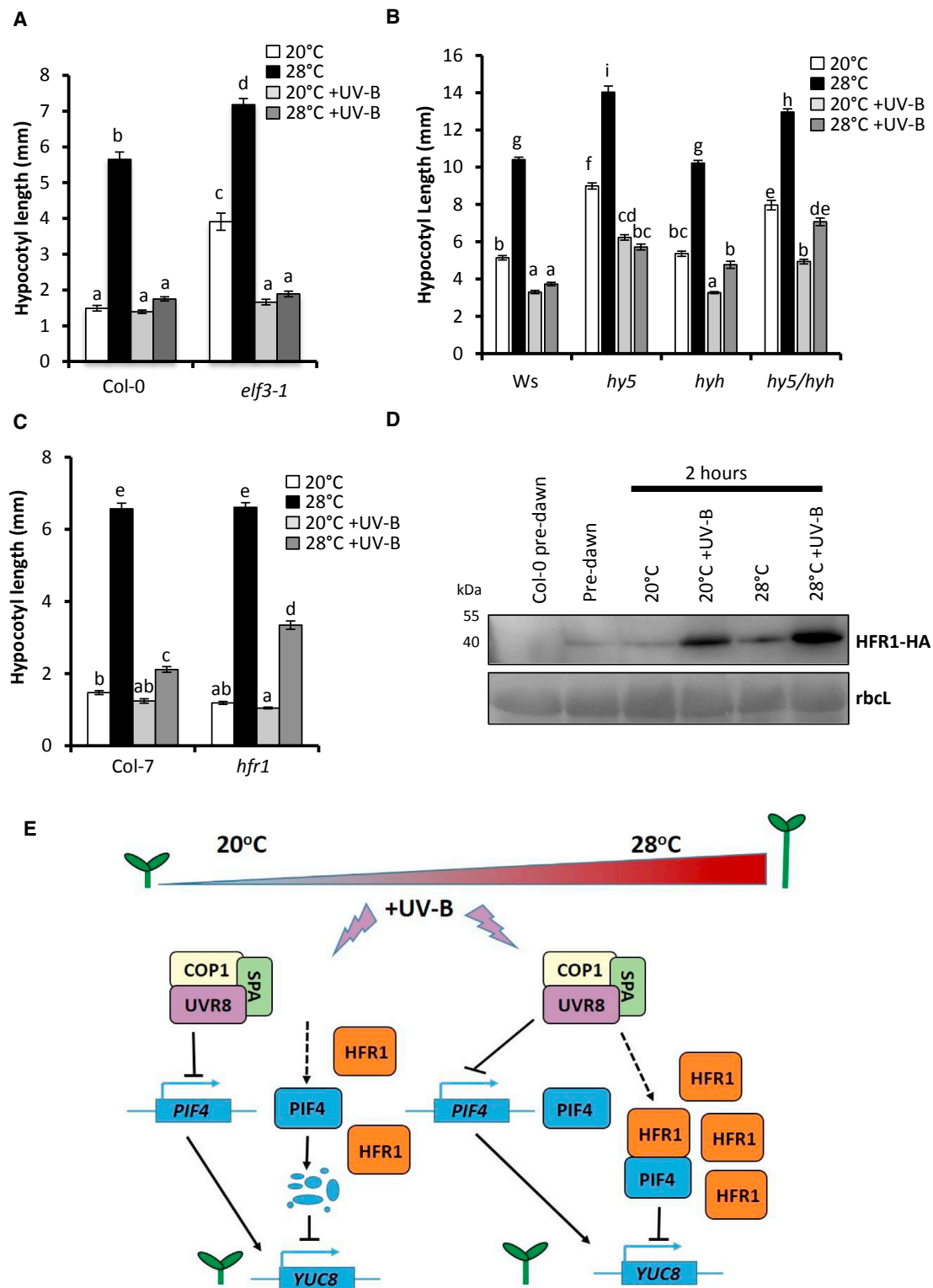


Figure 4. UV-B-Mediated Stabilization of HFR1 Suppresses PIF4 Activity at 28°C

(A–C) Hypocotyl lengths of (A) Col-0 and *elf3-1*; (B) Ws, *hy5*, *hyh*, and *hy5/hyh*; and (C) Col-7 and *hfr1* seedlings grown in continuous light for 3 days at 20°C, before transfer to 20°C, 28°C, 20°C + UV-B, or 28°C + UV-B for a further 4 days. Data represent mean values ($n = 40$) \pm SE. Different letters indicate statistically significant means ($p < 0.05$). Two-way ANOVA confirmed an interaction between genotype \times condition on hypocotyl length between Col-7 and *hfr1* plants ($p < 0.001$).

(D) Representative blot showing HFR1-HA abundance in *pHFR1::HFR1-HA* seedlings grown for 10 days in 16 hr light/8 hr dark cycles at 20°C, following 2 hr transfer to the stated conditions using an anti-HA antibody.

(legend continued on next page)

these conditions (Figure 4D). This assumption is supported by the reduced UV-B-mediated hypocotyl growth inhibition observed in *hfr1* mutants at 28°C (Figure 4C).

Elongation growth at high temperature may facilitate plant fitness through enhancing leaf cooling capacity [2–5]. Excessive stem growth at the expense of leaf and root development could, however, prove detrimental to plant survival, by critically reducing biomass and increasing lodging susceptibility. Our data suggest that enhanced UV-B absorption by leaves in direct sunlight would antagonize the effect of warming, thereby constraining stem elongation. It is therefore of particular relevance that daily peaks in UV-B and temperature coincide [16]. Caution must therefore be applied when interpreting thermomorphogenesis studies conducted in laboratory growth cabinets and glass-houses, which often contain little or no UV-B. Analysis of PIF function in natural canopies with fluctuating light and temperature conditions will be a key area of future research.

SUPPLEMENTAL INFORMATION

Supplemental Information includes Supplemental Experimental Procedures and four figures and can be found with this article online at <http://dx.doi.org/10.1016/j.cub.2016.11.004>.

AUTHOR CONTRIBUTIONS

S.H., A.S., and D.P.F. designed and performed experiments and analyzed data. C.K.C.-B. performed experiments. M.T. and E.T. provided new material and performed experiments. C.F. designed experiments and interpreted data. K.A.F. and G.I.J. supervised the project and wrote the manuscript together with S.H., A.S., and D.P.F.

ACKNOWLEDGMENTS

We thank Nicholas Harberd (University of Oxford) and Jaime Martinez-Garcia (CRAG, Barcelona) for seeds. We thank Patricia Hornitschek for initiating experiments with the HFR1-HA lines. S.H. was supported by a NERC studentship. D.P.F. is supported by a BBSRC CASE studentship with Vitacress. E.T. is supported by the Swiss National Science Foundation grant CRSII3_154438 to Roman Ulm (University of Geneva) and C.F. C.F. also acknowledges funding from the University of Lausanne. A.S. and C.K.C.-B. are supported by BBSRC grant BB/M008711/1 to K.A.F. and G.I.J.

Received: May 19, 2016

Revised: October 7, 2016

Accepted: November 1, 2016

Published: December 15, 2016

REFERENCES

- Quint, M., Delker, C., Franklin, K.A., Wigge, P.A., Halliday, K.J., and van Zanten, M. (2016). Molecular and genetic control of plant thermomorphogenesis. *Nat. Plants* 2, 15190.
- Gray, W.M., Östin, A., Sandberg, G., Romano, C.P., and Estelle, M. (1998). High temperature promotes auxin-mediated hypocotyl elongation in *Arabidopsis*. *Proc. Natl. Acad. Sci. USA* 95, 7197–7202.
- van Zanten, M., Voesenek, L.A.C.J., Peeters, A.J.M., and Millenaar, F.F. (2009). Hormone- and light-mediated regulation of heat-induced differential petiole growth in *Arabidopsis*. *Plant Physiol.* 151, 1446–1458.
- Crawford, A.J., McLachlan, D.H., Hetherington, A.M., and Franklin, K.A. (2012). High temperature exposure increases plant cooling capacity. *Curr. Biol.* 22, R396–R397.
- Bridge, L.J., Franklin, K.A., and Homer, M.E. (2013). Impact of plant shoot architecture on leaf cooling: a coupled heat and mass transfer model. *J. R. Soc. Interface* 10, 20130326.
- Koini, M.A., Alvey, L., Allen, T., Tilley, C.A., Harberd, N.P., Whitelam, G.C., and Franklin, K.A. (2009). High temperature-mediated adaptations in plant architecture require the bHLH transcription factor PIF4. *Curr. Biol.* 19, 408–413.
- Stavang, J.A., Gallego-Bartolomé, J., Gómez, M.D., Yoshida, S., Asami, T., Olsen, J.E., García-Martínez, J.L., Alabadi, D., and Blázquez, M.A. (2009). Hormonal regulation of temperature-induced growth in *Arabidopsis*. *Plant J.* 60, 589–601.
- Sun, J., Qi, L., Li, Y., Chu, J., and Li, C. (2012). PIF4-mediated activation of YUCCA8 expression integrates temperature into the auxin pathway in regulating *Arabidopsis* hypocotyl growth. *PLoS Genet.* 8, e1002594.
- Wang, R., Zhang, Y., Kieffer, M., Yu, H., Kepinski, S., and Estelle, M. (2016). HSP90 regulates temperature-dependent seedling growth in *Arabidopsis* by stabilizing the auxin co-receptor F-box protein TIR1. *Nat. Commun.* 7, 10269.
- Zheng, Z., Guo, Y., Novák, O., Chen, W., Ljung, K., Noel, J.P., and Chory, J. (2016). Local auxin metabolism regulates environment-induced hypocotyl elongation. *Nat. Plants* 2, 16025.
- Rizzini, L., Favory, J.-J., Cloix, C., Faggionato, D., O'Hara, A., Kaiserli, E., Baumeister, R., Schäfer, E., Nagy, F., Jenkins, G.I., and Ulm, R. (2011). Perception of UV-B by the *Arabidopsis* UVR8 protein. *Science* 332, 103–106.
- Foreman, J., Johansson, H., Hornitschek, P., Josse, E.M., Fankhauser, C., and Halliday, K.J. (2011). Light receptor action is critical for maintaining plant biomass at warm ambient temperatures. *Plant J.* 65, 441–452.
- Franklin, K.A., Toledo-Ortiz, G., Pyott, D.E., and Halliday, K.J. (2014). Interaction of light and temperature signalling. *J. Exp. Bot.* 65, 2859–2871.
- Ma, D., Li, X., Guo, Y., Chu, J., Fang, S., Yan, C., Noel, J.P., and Liu, H. (2016). Cryptochrome 1 interacts with PIF4 to regulate high temperature-mediated hypocotyl elongation in response to blue light. *Proc. Natl. Acad. Sci. USA* 113, 224–229.
- Pedmale, U.V., Huang, S.S., Zander, M., Cole, B.J., Hetzel, J., Ljung, K., Reis, P.A.B., Sridevi, P., Nito, K., Nery, J.R., et al. (2016). Cryptochromes interact directly with PIFs to control plant growth in limiting blue light. *Cell* 164, 233–245.
- Findlay, K.M.W., and Jenkins, G.I. (2016). Regulation of UVR8 photoreceptor dimer/monomer photo-equilibrium in *Arabidopsis* plants grown under photoperiodic conditions. *Plant Cell Environ.* 39, 1706–1714.
- Robson, T.M., Klem, K., Urban, O., and Jansen, M.A.K. (2015). Re-interpreting plant morphological responses to UV-B radiation. *Plant Cell Environ.* 38, 856–866.

(E) Hypothetical model depicting UV-B-mediated inhibition of hypocotyl elongation at different temperatures. At 20°C, UV-B perceived by UVR8 inhibits *PIF4* transcript accumulation in a response requiring COP1. This reduces *PIF4* protein abundance. Simultaneously, UV-B drives degradation of *PIF4* protein and stabilizes HFR1. At 28°C, UV-B perceived by UVR8 inhibits *PIF4* transcript abundance, in a response requiring COP1. This reduces *PIF4* protein accumulation. *PIF4* is protected from UV-B-induced degradation at elevated temperature, but its transcriptional activity is inhibited by high HFR1 levels. The abundance of HFR1 increases at 28°C. In UV-B, UVR8 sequesters COP1, inhibiting COP1-mediated HFR1 degradation. A role for HYH in the UV-B-mediated inhibition of hypocotyl elongation was additionally observed at high temperature, although no known mechanism exists for HYH regulation of *PIF4* activity. Collectively, UV-B inhibits hypocotyl elongation by reducing *PIF4* abundance and activity, thereby limiting auxin biosynthesis. The relative contributions of different regulatory mechanisms to this overall response are dependent on ambient temperature. See also Figures S2–S4.

18. Li, S.S., Wang, Y., and Björn, L.O. (2004). Effects of temperature on UV-B induced DNA damage and photorepair in *Arabidopsis thaliana*. *J. Environ. Sci. (China)* **16**, 173–176.
19. Takeuchi, Y., Ikeda, S., and Kasahara, H. (1993). Dependence on wavelength and temperature of growth inhibition induced by UV-B irradiation. *Plant Cell Physiol.* **34**, 913–917.
20. Delker, C., Sonntag, L., James, G.V., Janitza, P., Ibañez, C., Ziermann, H., Peterson, T., Denk, K., Mull, S., Ziegler, J., et al. (2014). The DET1-COP1-HY5 pathway constitutes a multipurpose signaling module regulating plant photomorphogenesis and thermomorphogenesis. *Cell Rep.* **9**, 1983–1989.
21. Box, M.S., Huang, B.E., Domijan, D., Jaeger, K.E., Khattak, A.K., Yoo, S.J., Sedivy, E.L., Jones, D.M., Hearn, T.J., Webb, A.A., et al. (2015). *ELF3* controls thermoresponsive growth in *Arabidopsis*. *Curr. Biol.* **25**, 194–199.
22. Mizuno, T., Nomoto, Y., Oka, H., Kitayama, M., Takeuchi, A., Tsubouchi, M., and Yamashino, T. (2014). Ambient temperature signal feeds into the circadian clock transcriptional circuitry through the EC night-time repressor in *Arabidopsis thaliana*. *Plant Cell Physiol.* **55**, 958–976.
23. Nusinow, D.A., Helfer, A., Hamilton, E.E., King, J.J., Imaizumi, T., Schultz, T.F., Farré, E.M., and Kay, S.A. (2011). The ELF4-ELF3-LUX complex links the circadian clock to diurnal control of hypocotyl growth. *Nature* **475**, 398–402.
24. Franklin, K.A., Lee, S.H., Patel, D., Kumar, S.V., Spartz, A.K., Gu, C., Ye, S., Yu, P., Breen, G., Cohen, J.D., et al. (2011). Phytochrome-interacting factor 4 (PIF4) regulates auxin biosynthesis at high temperature. *Proc. Natl. Acad. Sci. USA* **108**, 20231–20235.
25. Mashiguchi, K., Tanaka, K., Sakai, T., Sugawara, S., Kawaide, H., Natsume, M., Hanada, A., Yaeno, T., Shirasu, K., Yao, H., et al. (2011). The main auxin biosynthesis pathway in *Arabidopsis*. *Proc. Natl. Acad. Sci. USA* **108**, 18512–18517.
26. Won, C., Shen, X., Mashiguchi, K., Zheng, Z., Dai, X., Cheng, Y., Kasahara, H., Kamiya, Y., Chory, J., and Zhao, Y. (2011). Conversion of tryptophan to indole-3-acetic acid by TRYPTOPHAN AMINOTRANSFERASES OF ARABIDOPSIS and YUCCAs in *Arabidopsis*. *Proc. Natl. Acad. Sci. USA* **108**, 18518–18523.
27. Hayes, S., Velanis, C.N., Jenkins, G.I., and Franklin, K.A. (2014). UV-B detected by the UVR8 photoreceptor antagonizes auxin signaling and plant shade avoidance. *Proc. Natl. Acad. Sci. USA* **111**, 11894–11899.
28. de Lucas, M., Davière, J.M., Rodríguez-Falcón, M., Pontin, M., Iglesias-Pedraz, J.M., Lorrain, S., Fankhauser, C., Blázquez, M.A., Titarenko, E., and Prat, S. (2008). A molecular framework for light and gibberellin control of cell elongation. *Nature* **451**, 480–484.
29. Feng, S., Martinez, C., Gusmaroli, G., Wang, Y., Zhou, J., Wang, F., Chen, L., Yu, L., Iglesias-Pedraz, J.M., Kircher, S., et al. (2008). Coordinated regulation of *Arabidopsis thaliana* development by light and gibberellins. *Nature* **451**, 475–479.
30. O'Hara, A., and Jenkins, G.I. (2012). In vivo function of tryptophans in the *Arabidopsis* UV-B photoreceptor UVR8. *Plant Cell* **24**, 3755–3766.
31. Nieto, C., López-Salmerón, V., Davière, J.-M., and Prat, S. (2015). ELF3-PIF4 interaction regulates plant growth independently of the Evening Complex. *Curr. Biol.* **25**, 187–193.
32. Toledo-Ortiz, G., Johansson, H., Lee, K.P., Bou-Torrent, J., Stewart, K., Steel, G., Rodríguez-Concepción, M., and Halliday, K.J. (2014). The HY5-PIF regulatory module coordinates light and temperature control of photosynthetic gene transcription. *PLoS Genet.* **10**, e1004416.
33. Ulm, R., Baumann, A., Oravec, A., Máté, Z., Adám, E., Oakeley, E.J., Schäfer, E., and Nagy, F. (2004). Genome-wide analysis of gene expression reveals function of the bZIP transcription factor HY5 in the UV-B response of *Arabidopsis*. *Proc. Natl. Acad. Sci. USA* **101**, 1397–1402.
34. Brown, B.A., Cloix, C., Jiang, G.H., Kaiserli, E., Herzyk, P., Kliebenstein, D.J., and Jenkins, G.I. (2005). A UV-B-specific signaling component orchestrates plant UV protection. *Proc. Natl. Acad. Sci. USA* **102**, 18225–18230.
35. Oravec, A., Baumann, A., Máté, Z., Brzezinska, A., Molinier, J., Oakeley, E.J., Adám, E., Schäfer, E., Nagy, F., and Ulm, R. (2006). CONSTITUTIVELY PHOTOMORPHOGENIC1 is required for the UV-B response in *Arabidopsis*. *Plant Cell* **18**, 1975–1990.
36. Lee, H.-J., Jung, J.-H., Cortés Llorca, L., Kim, S.-G., Lee, S., Baldwin, I.T., and Park, C.-M. (2014). FCA mediates thermal adaptation of stem growth by attenuating auxin action in *Arabidopsis*. *Nat. Commun.* **5**, 5473.
37. Galstyan, A., Cifuentes-Esquível, N., Bou-Torrent, J., and Martínez-García, J.F. (2011). The shade avoidance syndrome in *Arabidopsis*: a fundamental role for atypical basic helix-loop-helix proteins as transcriptional cofactors. *Plant J.* **66**, 258–267.
38. Hornitschek, P., Lorrain, S., Zoete, V., Michielin, O., and Fankhauser, C. (2009). Inhibition of the shade avoidance response by formation of non-DNA binding bHLH heterodimers. *EMBO J.* **28**, 3893–3902.
39. Roig-Villanova, I., Bou-Torrent, J., Galstyan, A., Carretero-Paulet, L., Portolés, S., Rodríguez-Concepción, M., and Martínez-García, J.F. (2007). Interaction of shade avoidance and auxin responses: a role for two novel atypical bHLH proteins. *EMBO J.* **26**, 4756–4767.
40. Lorrain, S., Trevisan, M., Pradervand, S., and Fankhauser, C. (2009). Phytochrome interacting factors 4 and 5 redundantly limit seedling de-etiolation in continuous far-red light. *Plant J.* **60**, 449–461.

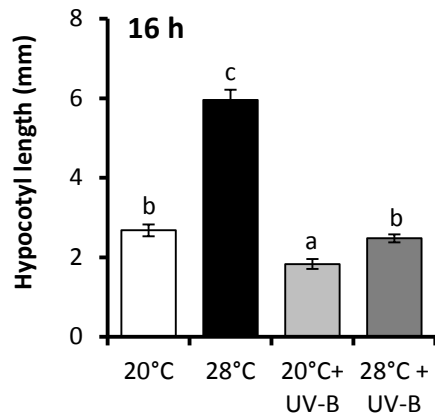
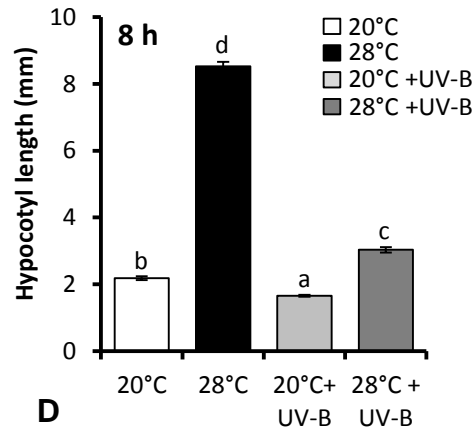
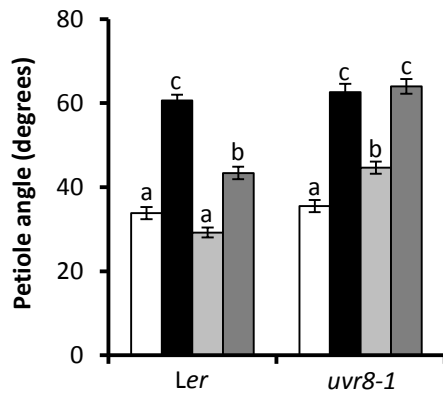
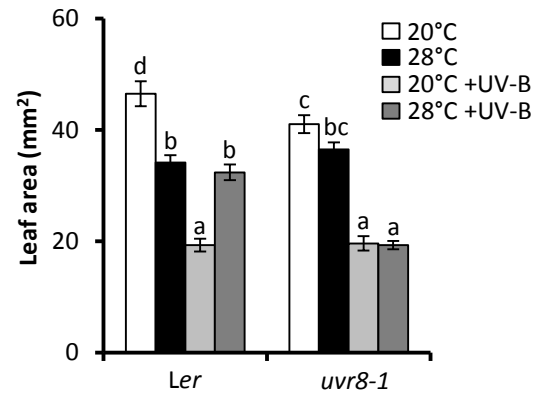
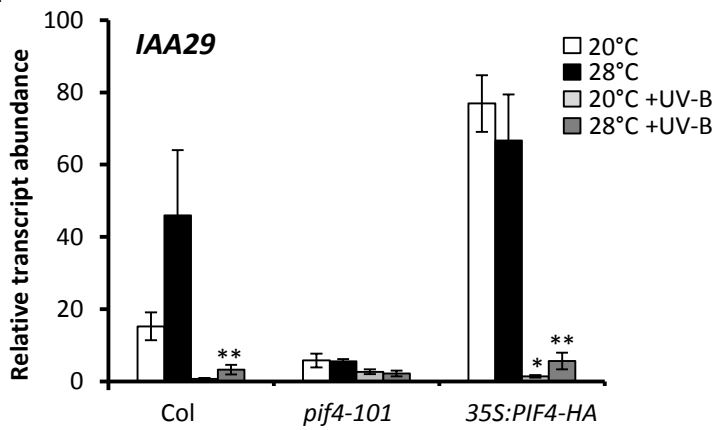
Current Biology, Volume 27

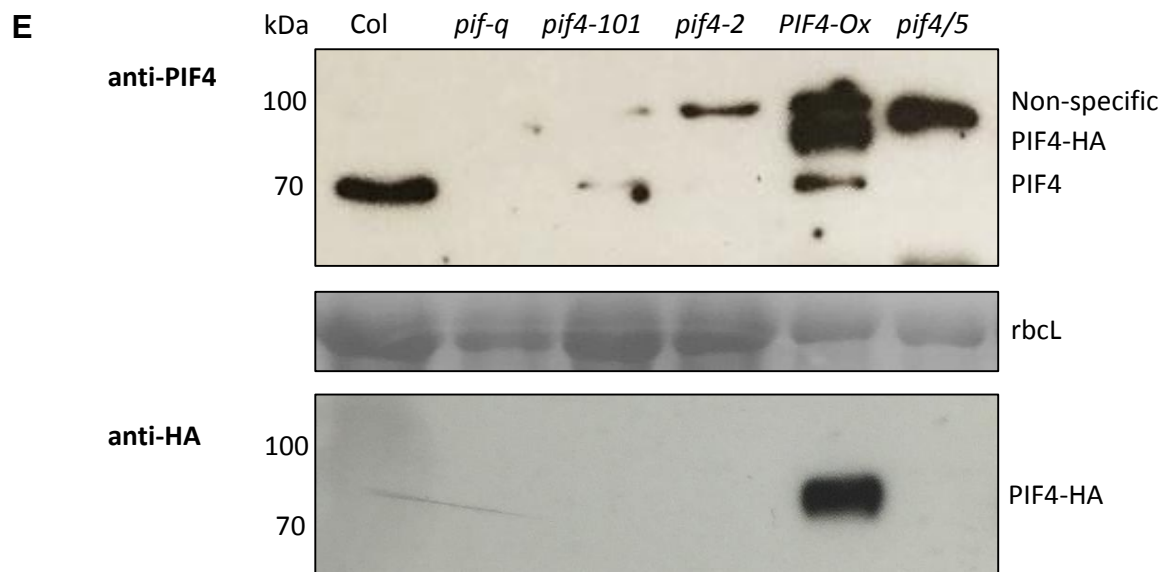
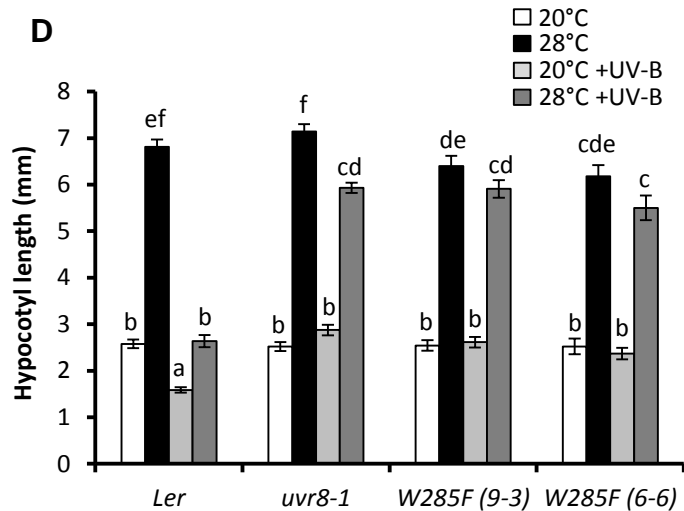
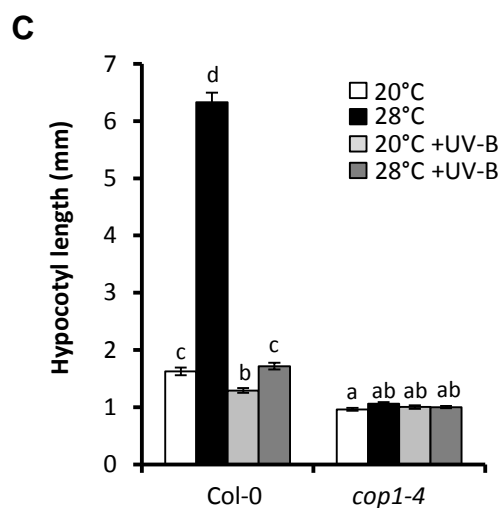
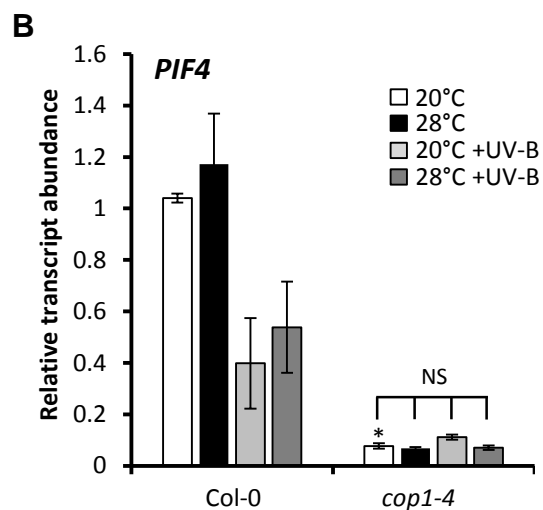
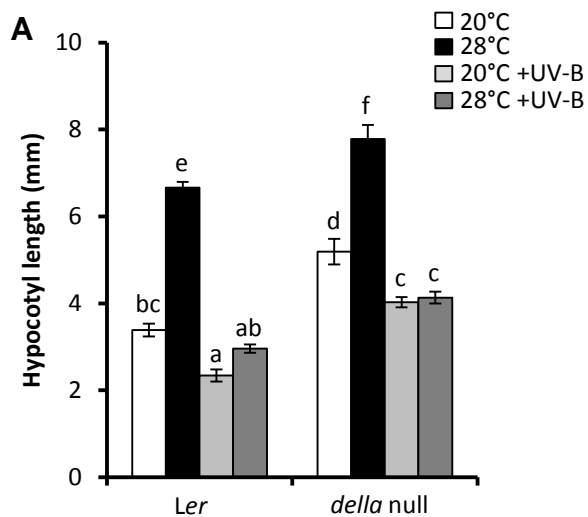
Supplemental Information

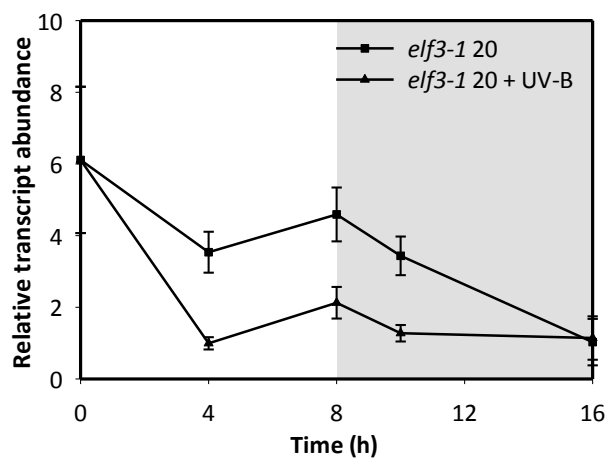
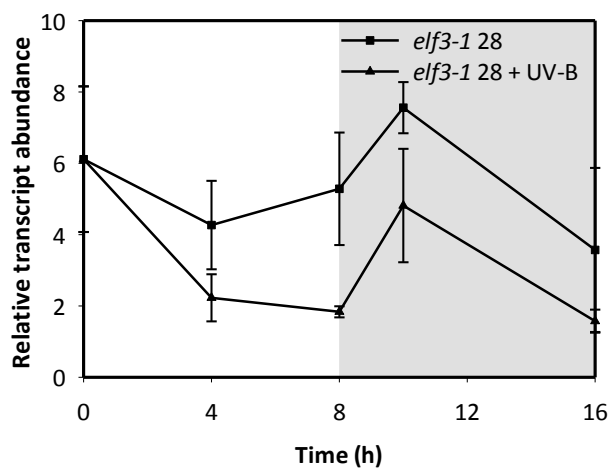
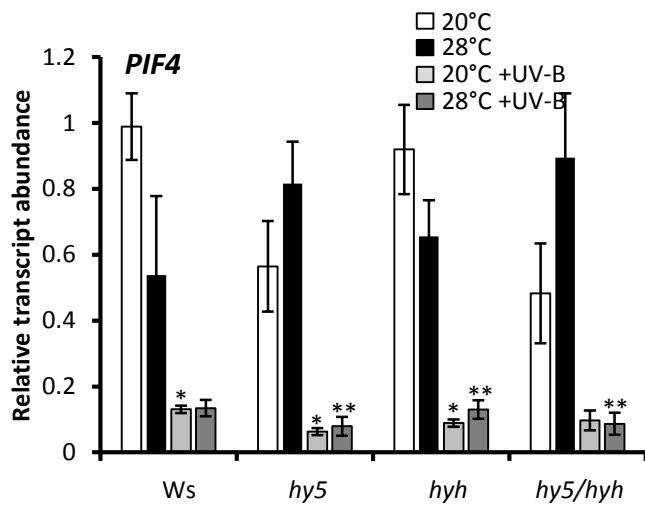
UV-B Perceived by the UVR8 Photoreceptor

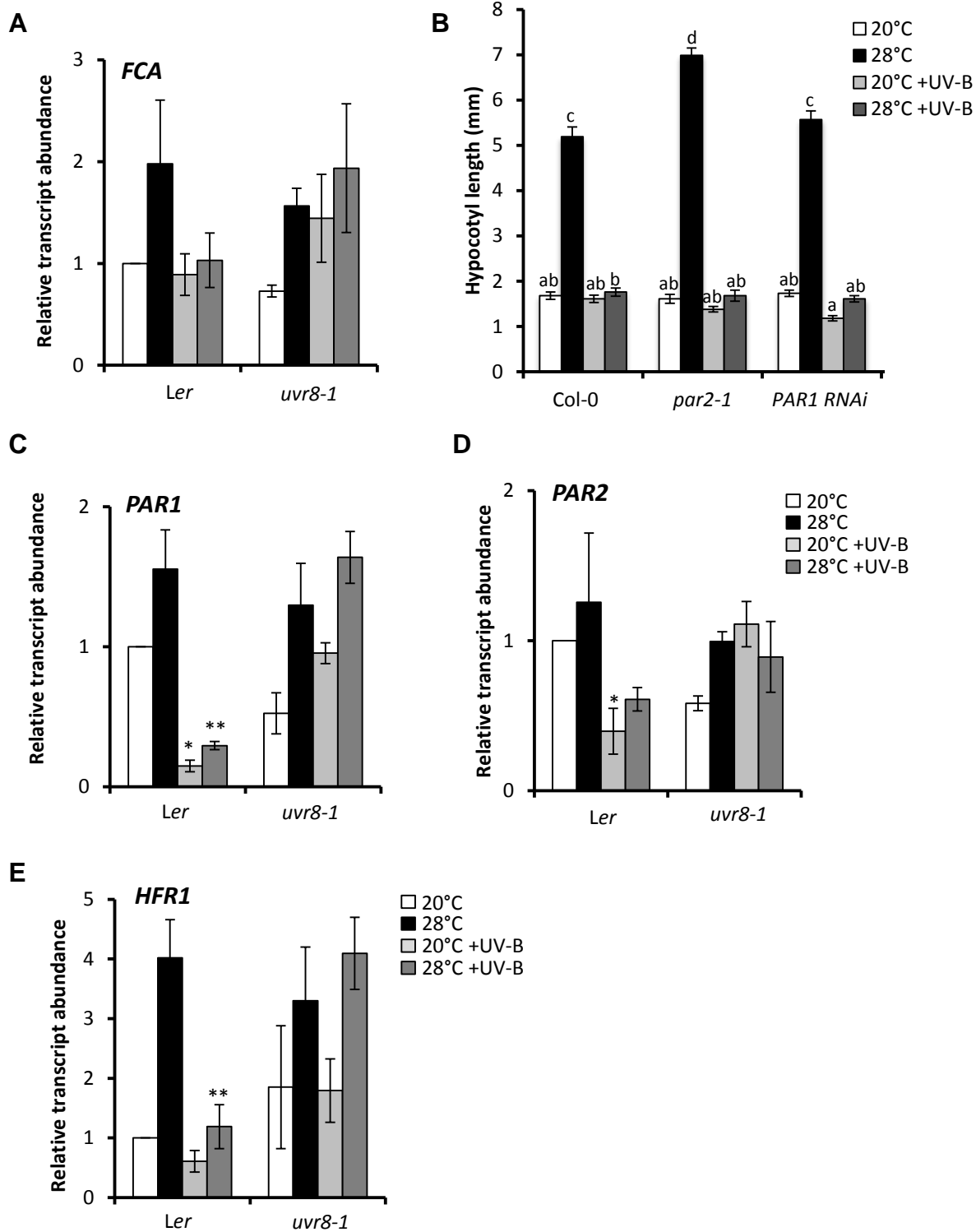
Inhibits Plant Thermomorphogenesis

Scott Hayes, Ashutosh Sharma, Donald P. Fraser, Martine Trevisan, C. Kester Cragg-Barber, Eleni Tavridou, Christian Fankhauser, Gareth I. Jenkins, and Keara A. Franklin

A**B****C****D****E**



A**B****C****D**



Supplemental Figure Legends

Figure S1, related to Figures 1 and 2. UV-B inhibits plant photomorphogenesis in multiple photoperiods. (A,B) Hypocotyl lengths of Col-0 seedlings grown in (A) 16 h light/ 8 h dark cycles and (B) 8 h light/ 16 h dark cycles for 3 d at 20°C, before transfer to 20°C, 28°C, 20°C +UV-B or 28°C +UV-B for a further 4 d. Data represent means ($n = 15$) \pm SE. Different letters indicate statistically significant means ($p < 0.05$). (C) Petiole angle from horizontal of *Ler* and *uvr8-1* plants grown in 16 h light/ 8 h dark cycles for 10 d at 20°C before transfer to 20°C, 28°C, 20°C +UV-B or 28°C +UV-B for a further 8 d. Data represent mean ($n=24$) \pm SE. (D) Leaf area of leaf 4 of plants grown as in (C) 9 d after transfer. Data represent mean ($n \geq 23$) \pm SE. Different letters indicate statistically significant means ($p < 0.05$). (E) Relative transcript abundance of *IAA29* in Col-0, *pif4-101* and *PIF4ox* seedlings grown for 10 d in a 16 h photoperiod at 20°C, before transfer at dawn to the indicated conditions for 4 h. $n=3 \pm$ SE. *Significant UV-B-mediated decrease in transcript abundance when compared to 20°C ($p < 0.05$). **Significant UV-B-mediated decrease in transcript abundance when compared to 28°C ($p < 0.05$).

Figure S2, related to Figures 3 and 4. UV-B-mediated suppression of high temperature-induced hypocotyl elongation is not mediated by DELLA proteins and COP1 promotes PIF4 expression. (A) Hypocotyl lengths of *Ler* and *della* null seedlings grown in continuous light for 3 d at 20°C, before transfer to 20°C, 28°C, 20°C +UV-B or 28°C +UV-B for a further 4 d. Data represent means ($n \geq 19$) \pm SE. Different letters indicate statistically significant means ($p < 0.05$). 2-way ANOVA confirmed there was no significant interaction between genotype and condition on hypocotyl length ($p > 0.1$). (B) Relative transcript abundance of *PIF4* in Col-0 and *cop1-4* seedlings grown for 10 days in 16 h light/ 8 h dark cycles at 20°C, before transfer at dawn to the indicated conditions for 4 h. $n=3 \pm$ S.E. *Significant decrease in transcript abundance when compared to Col-0 in identical conditions ($p < 0.05$). NS = No significant difference in *PIF4* transcript abundance between indicated treatments ($p < 0.05$). (C) Hypocotyl lengths of Col-0 and *cop1-4* seedlings grown in continuous light for 3 d at 20°C, before transfer to 20°C, 28°C, 20°C +UV-B or 28°C +UV-B for a further 4 d. $n=35 \pm$ SE. Different letters indicate statistically significant means ($p < 0.05$). (D) Hypocotyl lengths of *Ler*, *uvr8-1* and two independent lines of *uvr8-1*/GFP-UVR8^{W285F} (*W285F*), were grown in continuous light for 3 d at 20°C, before transfer to 20°C, 28°C, 20°C +UV-B or 28°C +UV-B for a further 4 d. $n \geq 10 \pm$ SE. Different letters indicate statistically significant means ($p < 0.05$). (E) PIF4 and PIF4-HA abundance in WT, PIF4-deficient mutants (*pif-q*, *pif4-101*, *pif4-2* and *pif4/5*) and *PIF4-HA* overexpressor plants grown for 10 d in 16 h light/ 8 h dark cycles at 20°C and harvested before dawn. The blot was probed with anti-PIF4, stripped and re-probed with anti-HA. Ponceau stain of Rubisco large subunit (rbcl) serves as a loading control.

Figure S3, related to Figure 3 and 4. UV-B-mediated suppression of high temperature-induced hypocotyl elongation is not mediated by ELF3 or HY5. (A,B) Time course of *PIF4* transcript abundance in *elf3-1* mutants. Seedlings were grown for 10 d in 8 h light/16 h dark cycles at 20°C. On day 11, plants were transferred to either 20°C or 28°C \pm UV-B. UV-B treatment was maintained for the duration of the photoperiod and plants harvested at the times shown. All values are normalized to Col-0 at time 0. The mean of 2 biological repeats are shown \pm SE. (C) Col-0 and *elf3-1* seedlings grown in continuous light for 3 d at 20°C, before transfer to 20°C, 28°C, 20°C +UV-B or 28°C +UV-B for a further 4 d. (D) Relative transcript abundance of *PIF4* in *Ws*, *hy5*, *hyh* and *hy5/hyh* seedlings grown for 10 d in 16 h light/ 8 h dark cycles at 20°C, before transfer at dawn to the indicated conditions for 4 h. $n=3 \pm$ SE. *Significant UV-B-mediated decrease in transcript abundance when compared to 20°C ($p < 0.05$). **Significant UV-B-mediated decrease in transcript abundance when compared to 28°C ($p < 0.05$).

Figure S4, related to Figure 4. UV-B does not increase transcript abundance of FCA, PAR1, PAR2 or HFR1. (A) Relative transcript abundance of *FCA* in *Ler* and *uvr8-1* seedlings grown for 10 d in a 16 h light/ 8 h dark cycles at 20°C, before transfer at dawn to the indicated conditions for 4 h. $n=3 \pm$ SE. (B) Hypocotyl lengths of the *par2-1* mutant and *PAR1*-RNAi line grown in continuous light for 3 d at 20°C, before transfer to 20°C, 28°C, 20°C +UV-B or 28°C +UV-B for a further 4 d. Data represent means ($n \geq 19$) \pm SE. Different letters indicate statistically significant means ($p < 0.05$). (C) Relative transcript of *PAR1*, (D) *PAR2* and (E) *HFR1* grown as in (A). *Significant UV-B-mediated decrease in transcript abundance when compared to 20°C ($p < 0.05$). **Significant UV-B-mediated decrease in transcript abundance when compared to 28°C ($p < 0.05$).

Supplemental Experimental Procedures

Plant material

All mutants and transgenic lines used in this study have been described previously. The *uvr8-1* [S1] and the *della* null [S2] mutants are in the Landsberg *erecta* (*Ler*) background. The *hy5KS50* [S3], *hyh* [S4] and *hy5KS50/hyh* mutants [S4] are in the Wassilewskija (*Ws*) background. The *PIF4-HA* over-expressor, *pif4-101* and *pif4/5* lines [S5], *PAR1-RNAi* and *par2-1* lines [S6], *pif4-2* and *pif-q* mutants [S7], *elf3-1* [S8] and *cop1-4* [S9] mutants are in the Columbia (*Col-0*) background. *uvr8-1/GFP-UVR8^{W285F}* lines are in the *Ler* background [S10]. The *hfr1-101* mutant is in the *Col-7* background [S11]. pPH73 (*HFR1pro:HFR1-3XHA*) was constructed by amplifying 2.1kb 5' of the *HFR1* ATG using primers 5'-tgactctagaggtaccggcgatcgctacgaaaagaagaag-3' and 5'-gtcaggatccttagttaagagatcggagatga-3'. *HFR1* cDNA with a triple HA tag at the C-terminus was amplified from vector pCF396 described in [S12]. *HFR1* promoter and cDNA were ligated into pPZP211 including an *RBCS* terminator sequence 3' of the *HFR1* gene. This construct was transformed into *hfr1-101* and lines with a single insertion site that complemented the *hfr1* phenotype were selected.

Growth conditions

Seeds were sown directly onto a 3:1 mixture of compost: horticultural silver sand. After 4 d stratification in darkness at 4°C, seedlings were germinated in controlled growth cabinets (Microclima 1600E, Snijder Scientific) in continuous white light at 20°C and 70% humidity. Plants were either left in control cabinets or transferred to the indicated conditions at the specified time. For adult plant experiments, qPCR analysis and western blots, plants were grown in the same cabinets under 16 h light/8 h dark cycles or 8 h light/ 16 h dark cycles. White light was provided by cool-white fluorescent tubes (400-700 nm) at a photon irradiance of 90 $\mu\text{mol m}^{-2}\text{s}^{-1}$. Supplementary narrowband UV-B was provided at a photon irradiance of 400 mW m^{-2} (approximately 1 $\mu\text{mol m}^{-2}\text{s}^{-1}$) by Philips TL100W/01 tubes. UV-B levels were modulated by strips of heat-proof tape. Biologically effective UV-B dose (BE-UV-B) was calculated 3.6 $\mu\text{W m}^{-2}\text{nm}^{-1}$, following Flint and Caldwell [S13]. Control conditions also contained the same UV-B tubes, with an extruded acrylic cover which selectively blocked UV wavelengths. All light measurements were performed using an Ocean Optics FLAME-S-UV-VIS spectrometer with a cosine corrector (oceanoptics.com).

Plant measurements

Measurements of hypocotyl length, petiole length, leaf angle and leaf area were recorded using ImageJ software (<http://www.rsb.info.gov/ij>). For hypocotyl measurements, a minimum of 15 seedlings were measured for each genotype in each condition. For leaf area and petiole length measurements, the largest fully expanded rosette leaf (leaf 4) was excised from each plant at day 19. Leaf angles of leaf 4 were measured from the horizontal soil surface at day 18. Measurements were recorded from a minimum of 23 plants per treatment. At least two biological repeats were performed for each experiment with similar results.

RNA extraction and qPCR analysis.

Seedlings were initially grown in control conditions under 16 h light/ 8 h dark cycles for 10 d, before transfer at dawn to different light and temperature conditions for the indicated time. RNA extraction, cDNA synthesis and qPCR were performed as described previously [S14]. Transcript abundance values were normalised to *ACTIN2*. See list of primers for *ACTIN2*, *FCA*, *HFR1*, *IAA29*, *PAR1*, *PAR2*, *PIF4*, and *YUCCA8* sequences. Three biological replicates were performed for each experiment. For time course analyses, 2 biological repeats were performed with similar results.

Protein extraction and western blotting

Seedlings were grown in 16 h light/ 8 h dark photoperiods for 10 d at 20°C, before transfer at dawn to different light and temperature conditions for the indicated time. Samples were harvested into liquid nitrogen and extracted in buffer (100 mM tris-HCl (pH 8), 4 M urea, 5% (w/v) SDS, 15% (v/v) glycerol, 10 mM β -ME, 30 $\mu\text{l/ml}$ protease inhibitor cocktail (Sigma)), before boiling at 95°C for 4 min and centrifugation at maximum speed for 15 min. Protein levels were quantified by RC DC Lowry assay (Biorad). SDS-PAGE sample buffer (4x (8% (w/v) SDS, 0.4% (w/v) bromophenol blue, 40% (v/v) glycerol, 200 mM tris-HCl (pH6.8), 400 mM β -ME)) was added to supernatants to a final dilution of 1x. Samples were then heated for 5 min at 95°C.

For PIF4-HA immunoblots, 30 μg of total protein was loaded on to 10% SDS-PAGE gels and blotted on to nitrocellulose membranes (Biorad). Membranes were incubated overnight at 4°C in 1:1000 anti-HA antibody conjugated to peroxidase (Roche). Signals were detected using ECL2 (Thermo Scientific). Blots were performed in triplicate at each time point. Band intensity was analysed with ImageJ. Protein abundance was normalised to ponceau staining of rubisco large subunit and expressed as a value relative to pre-dawn levels.

For native PIF4 and HFR1 immunoblots, protein extracts (70 μg for PIF4 or 40 μg for HFR1-HA) were separated on 10% or 12% SDS-PAGE gels, respectively and blotted on PVDF membrane (Thermo Scientific). Membranes were incubated overnight at 4°C in 1:1000 anti-PIF4 (Agrisera) or 1:2000 anti-HA (Covance). Secondary antibody incubations were performed for 1 h at room temperature using 1:10000 anti-rabbit (Promega) or 1:5000 anti-mouse (Dako) antibodies conjugated with peroxidase. Signals were detected using the SuperSignalTM West Femto Maximum Sensitivity Substrate (Thermo Scientific). Protein abundance was normalised to ponceau staining of rubisco large subunit.

Statistical analyses

Statistical analyses were carried out using IBM SPSS Statistics 21.0 software. Morphological assays were analyzed using a one-way ANOVA, treating genotype and temperature/light condition together as a single factor. Tukey's post-hoc tests were used to deduce statistically significant means ($p < 0.05$) as indicated by letters in the figures. For selected experiments 2-way ANOVAs were performed to either confirm or rule-out interactions between genotypes and conditions. For qPCR analyses, relative expression values were first transformed by Log2. Student's t-tests were then performed to investigate differences between the means indicated in the figure legends ($p < 0.05$). Student's t-test was also performed to analyse quantitative western blot data.

Primer sequences used for qPCR

Primer	Sequence
<i>ActinF</i>	TCAGATGCCCAGAAGTGTGTTCC
<i>ActinR</i>	CCGTACAGATCCTTCCTGATATCC
<i>FCAF</i>	GCTCTTGTCGCAGCAAATC
<i>FCAR</i>	GATCCAGCCCAGTGTGTTTAC
<i>HFR1F</i>	TAAATTGGCCATTACCACCGTTTA
<i>HFR1R</i>	ACCGTGAAGAGACTGAGGAGAAGA
<i>IAA29F</i>	ATCACCATCATTGCCCGTAT
<i>IAA29R</i>	ATTGCCACACCATCCATCTT
<i>PAR1F</i>	CACGAGACGCTCTCTGT
<i>PAR1R</i>	TTCTCGGTCTTCACGTAC
<i>PAR2F</i>	CGTAGAAGATGAAGATGAA
<i>PAR2R</i>	CGTAGTAAGAACTTTAATGG
<i>PIF4F</i>	GCCGATGGAGATGTTGAGAT
<i>PIF4R</i>	CCAACCTAGTGGTCCAAACG
<i>YUCCA8F</i>	ATCAACCCTAAGTTCAACGAGTG
<i>YUCCA8R</i>	CTCCCGTAGCCACCACAAG

Supplemental References

- S1. Kliebenstein, D., Lim, J., Landry, L., and Last, R. (2002) Arabidopsis UVR8 regulates Ultraviolet-B signal transduction and tolerance and contains sequence similarity to Human Regulator of Chromatin Condensation 1. *Plant Physiol.* *130*, 234–43.
- S2. Koini, M.A., Alvey, L., Allen, T., Tilley, C.A., Harberd, N.P., Whitlam, G.C., and Franklin, K.A. (2009). High Temperature-Medated Adaptations in Plant Architecture Require the bHLH Transcription Factor PIF4. *Curr. Biol.* *19*, 408–413.
- S3. Oyama, T., Shimura, Y., and Okada, K. (1997) The Arabidopsis HY5 gene encodes a bZIP protein that regulates stimulus-induced development of root and hypocotyl. *Genes Dev.* *11*, 2983–95.
- S4. Holm, M., Ma, L., Qu, L., and Deng, X-W (2002) Two interacting bZIP proteins are direct targets of COP1-mediated control of light-dependent gene expression in Arabidopsis. *Genes Dev.* *16*, 1247–59.
- S5. Lorrain, S., Allen, T., Duek, P., Whitlam, G.C., and Fankhauser C. (2008) Phytochrome-mediated inhibition of shade avoidance involves degradation of growth-promoting bHLH transcription factors. *Plant J.* *53*, 312–23.

- S6. Roig-Villanova, I., Bou-Torrent, J., Galstyan, A., Carretero-Paulet, L., Portolés, S., Rodríguez-Concepción, M. and Martínez-García, J.F. (2007). Interaction of shade avoidance and auxin responses: a role for two novel atypical bHLH proteins. *EMBO J.* 26, 4756-4767.
- S7. Leivar, P., Monte, E., Oka, Y., Liu, T., Carle, C., Castillon, A., Huq, E. and Quail, P.Q. (2008). Multiple phytochrome-interacting bHLH transcription factors repress premature seedling photomorphogenesis in darkness. *Curr. Biol.* 18, 1815–1823.
- S8. Liu, X., Covington, M., Fankhauser, C., Chory, J. and Wagner, D. (2001) ELF3 encodes a circadian clock-regulated nuclear protein that functions in an Arabidopsis PHYB signal transduction pathway. *Plant Cell* 13, 1293–304.
- S9. McNellis, T., von Arnim, A., Araki, T., Komeda, Y., Miséra, S., and Deng, X. (1994) Genetic and molecular analysis of an allelic series of cop1 mutants suggests functional roles for the multiple protein domains. *Plant Cell* 6, 487–500.
- S10. O'Hara, A., and Jenkins, G.I. (2013) In vivo function of tryptophans in the Arabidopsis UV-B photoreceptor UVR8. *Plant Cell* 24, 3755-3766.
- S11. Duek, P. and Fankhauser, C. (2003) HFR1, a putative bHLH transcription factor, mediates both phytochrome A and cryptochrome signalling. *Plant J.* 34, 827–36.
- S12. Duek P.D., Elmer, M.V., van Oosten, V.R., Fankhauser, C. (2004) The Degradation of HFR1, a Putative bHLH Class Transcription Factor Involved in Light Signaling, Is Regulated by Phosphorylation and Requires COP1. *Current Biology* 14, 2296–2301.
- S13. Flint, S., and Caldwell, M. (2003) A biological spectral weighting function for ozone depletion research with higher plants. *Physiol. Plant.* 117, 137–44.
- S14. Salter M.G., Franklin, K.A., Whitelam, G.C. (2003) Gating of the rapid shade-avoidance response by the circadian clock in plants. *Nature* 426, 1–4.